Article

Characterization of Subdomain IIA Binding Site of Human Serum Albumin in its Native, Unfolded, and Refolded States Using Small Molecular Probes

Osama K. Abou-Zied, and Othman I. K. Al-Shihi

J. Am. Chem. Soc., **2008**, 130 (32), 10793-10801 • DOI: 10.1021/ja8031289 • Publication Date (Web): 19 July 2008

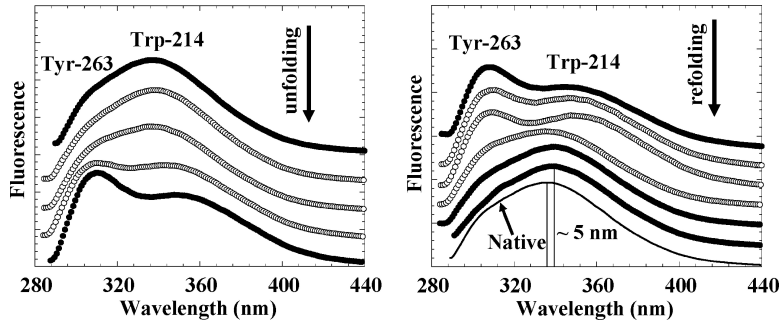

More About This Article

Additional resources and features associated with this article are available within the HTML version:

- Supporting Information
- Access to high resolution figures
- Links to articles and content related to this article
- Copyright permission to reproduce figures and/or text from this article

View the Full Text HTML

J|A|C|S
ARTICLES

Published on Web 07/19/2008

Characterization of Subdomain IIA Binding Site of Human Serum Albumin in its Native, Unfolded, and Refolded States Using Small Molecular Probes

Osama K. Abou-Zied* and Othman I. K. Al-Shihi

Department of Chemistry, Faculty of Science, Sultan Qaboos University, P.O. Box 36, Postal Code 123, Muscat, Sultanate of Oman

Received April 28, 2008; E-mail: abouzied@squ.edu.om

Abstract: Subdomain IIA binding site of human serum albumin (HSA) was characterized by examining the change in HSA fluorescence in the native, unfolded, and refolded states. The study was carried out in the absence and presence of small molecular probes using steady-state and time-resolved fluorescence measurements. 2-Pyridone, 3-pyridone, and 4-pyridone bear similar molecular structures to those found in many drugs and are used here as probes. They are found to specifically bind in subdomain IIA and cause a reduction in the fluorescence intensity and lifetime of the Trp-214 residue in native HSA which is located in the same subdomain. The efficiency of energy transfer from Trp-214 fluorescence to the probes was found to depend on the degree of the spectral overlap between the donor's fluorescence and the acceptor's absorption. After probe binding in subdomain IIA, the distance between the donor and acceptor was calculated using Förster theory. The calculated quenching rate constants and binding constants were also shown to depend on the degree of spectral overlap. The results point to a static quenching mechanism operating in the complexes. Denaturation of HSA in the presence of guanidine hydrochloride (GdnHCl) starts at [GdnHCl] > 1.0 M and is complete at [GdnHCl] ≥ 6.0 M. Upon unfolding, two fluorescence peaks were observed. One peak was assigned to the fluorescence of Trp-214 in a polar environment, and the other peak was assigned to tyrosine fluorescence. A reduction of the fluorescence intensity of the two peaks upon binding of the probes to the denatured HSA indicates that Tyr-263 in subdomain IIA is one of the tyrosine residues responsible for the second fluorescence peak. The results were confirmed by measuring the fluorescence spectra and lifetimes of denatured HSA at different excitation wavelengths, and of L-tryptophan and L-tyrosine free in buffer. The measured lifetimes of denatured HSA are typical of tryptophan in a polar environment and are slightly reduced upon probe binding. Dilution of the denatured HSA by buffer results in a partial refolding of subdomain IIA. This partial refolding is attributed to some swelling of the binding site caused by water. The swelling prevents a full recovery from the denatured state.

Introduction

Human serum albumin (HSA) is the most abundant protein in plasma and constitutes approximately half of the protein found in human blood.[1] This protein of 585 residues is composed of a single polypeptide chain,[2,3] with three α-helical domains I−III, each containing two subdomains A and B (Figure 1). The protein is stabilized by 17 disulfide bridges. The crystal structure analyses indicate that the principal regions of ligand binding sites in albumin are located in hydrophobic cavities in subdomains IIA and IIIA. These binding sites are known as Sudlow I and Sudlow II, respectively,[4,5] and the sole tryptophan residue in HSA is located in Sudlow I (Trp-214).[6]

HSA plays an important role in the transport and disposition of endogenous and exogenous ligands present in blood.[7] Its surprising capacity to reversibly bind a large variety of drugs results in its prevailing role in drug pharmacokinetics and pharmacodynamics.[8–10] Hence, it is important to characterize the binding sites of HSA by studying its interaction with varieties of relevant compounds.

In the present paper we use three isomers of small aromatic molecules as probes to characterize the binding sites in HSA. 2-Pyridone (2Py), 3-pyridone (3Py), and 4-pyridone (4Py) (shown in Figure 2) have received much interest due to the similarity of their molecular structures with those found in a wide range of drugs of different pharmacological functions.[11] The three probes have the same functional groups and similar

(1) Berde, C. B.; Hudson, B. S.; Simon, R. D.; Sklar, L. A. *J. Biol. Chem.* **1979**, *254*, 391–400.
(2) He, X. M.; Carter, D. C. *Nature* **1992**, *358*, 209–215.
(3) Dugaiczyk, A.; Law, S. W.; Dennison, O. E. *Proc. Natl. Acad.Sci. U.S.A.* **1982**, *79*, 71–75.
(4) Sudlow, G.; Birkett, D. J.; Wade, D. N. *Mol. Pharmacol.* **1975**, *11*, 824–832.
(5) Sudlow, G.; Birkett, D. J.; Wade, D. N. *Mol. Pharmacol.* **1976**, *12*, 1052–1061.
(6) Colmenarejo, G. *Med. Res. Rev.* **2003**, *23*, 275–301.
(7) Carter, D. C.; Ho, J. X. *Adv. Protein Chem.* **1994**, *45*, 153–203.
(8) Kragh-Hansen, U. *Pharmacol. Rev.* **1981**, *33*, 17–53.
(9) Peters, T. *Adv. Protein Chem.* **1985**, *37*, 61–245.
(10) Jusko, W. J.; Gretch, M. *Drug Metab. Rev.* **1976**, *5*, 43–140.
(11) El Gezawi, S.; Omar, N.; E1 Rabbat, N.; Ueda, H.; Perrin, J. H. *J. Pharm. Biomed. Anal.* **1988**, *6*, 399–406.

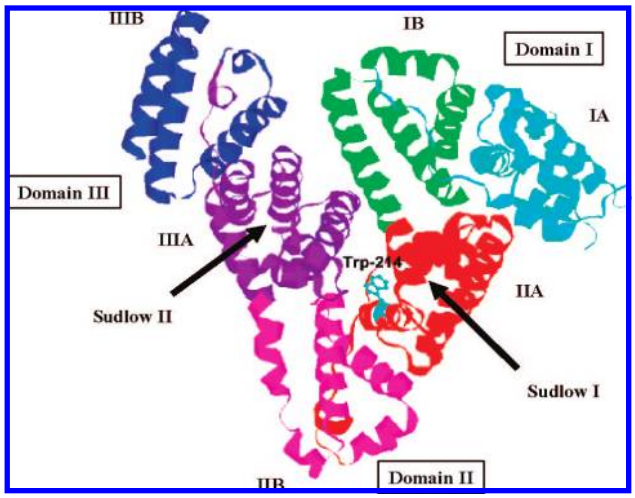

Figure 1. Crystal structure of HSA and the locations of domain-binding sites. The locations of hydrophobic binding sites (Sudlow I and Sudlow II) are indicated. The position of the tryptophan residue (Trp-214) in the middle of helix H2 in subdomain IIA is shown. The structure was obtained from the Protein Data Bank (ID code 1ha2).

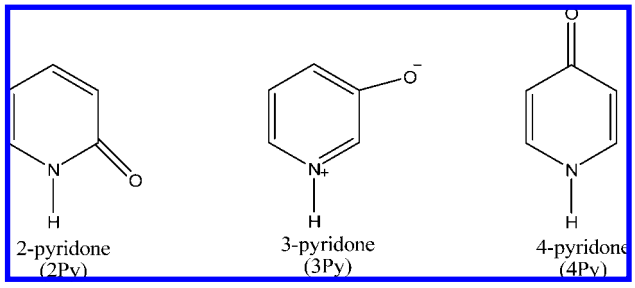

Figure 2. Structures of the probes.

chemical properties, which include the possibility of keto−enolic tautomerism (solvent polarity dependent).[12–20] However, their absorption spectra in water are very different where 3Py shows an absorption peak at $\lambda_{max} = 315$ nm due to the zwitterionic tautomer. In 2Py, the first absorption peak occurs at $\lambda_{max} = 295$ nm, and in 4Py, the first absorption peak is at $\lambda_{max} = 254$ nm. The wide difference in the absorption behavior of the three pyridones gives a unique opportunity to investigate the efficiency of energy transfer from the lone tryptophan residue in HSA to the probes using Förster resonance energy transfer (FRET).

In this work, we employ steady-state and time-resolved fluorescence measurements in order to obtain information related to the binding mechanisms of the probes to HSA such as binding modes, binding constants, binding sites, intermolecular distances, and quenching rate constants. We show that the probes bind specifically in Sudlow site I. We also investigate chemical unfolding and dilution refolding of HSA in the absence and presence of the probes. We show that binding of the probes in HSA reveals the assignment of a tyrosine residue responsible for the additional fluorescence component in the unfolded protein.

Experimental Section

HSA (essentially fatty acid free) and guanidine hydrochloride (GdnHCl) (8 M in H_2O (filtered)) were purchased from Sigma. L-Tryptophan (99%) and L-tyrosine (98.5%) were obtained from BDH Chemicals. 2Py (97%), 3Py (98%), and 4Py (95%) probes were obtained from Aldrich and were used without further purification. The buffer used was 50 mM sodium phosphate buffer, pH 7.2, and was obtained from Aldrich. The concentration of HSA in the buffer was prepared using its listed molecular weight of 66.5 kDa, and the final concentration was checked by comparing the measured absorbance with the published value (optical absorbance at 279 nm = 0.531 (1 g/L)).[21] For FRET experiments, the concentration of HSA and the probes was kept at 0.1 mM. For the determination of the quenching rate constants and binding constants, the concentration of HSA was 0.1 mM and that of the probes was varied in the range of 0.0−0.1 mM. For the unfolding experiments, the concentration of GdnHCl was varied by dilution in the said buffer, while keeping HSA concentration constant at 0.1 mM. For the refolding experiments, the start solution of 0.1 mM HSA and 8.0 M GdnHCl was diluted in buffer until final concentrations of 2.0 μM (HSA) and 0.1 M (GdnHCl). All prepared solutions were kept to equilibrate for 2 h before taking the measurements. Measurements were then repeated after 12 h, and no significant differences were detected.

Absorption spectra were obtained with an HP 845x diode array spectrophotometer. Fluorescence spectra were recorded on a Shimadzu RF-5301 PC spectrofluorophotometer. Lifetime measurements were performed using a TimeMaster fluorescence lifetime spectrometer obtained from Photon Technology International. Excitation was at 280, 295, and 310 nm using LEDs. The system response time as measured from the scattered light was estimated to be approximately 1.5 ns (fwhm). The measured transients were fitted to multiexponential functions convoluted with the system response function. The experimental time resolution (after deconvolution) was approximately 100 ps. In all the experiments, samples were contained in a 1 cm path length quartz cell and the measurements were conducted at 23 ± 1 °C.

Results and Discussion

Binding Mechanisms of 2Py, 3Py, and 4Py in HSA. HSA has three fluorophores which are tryptophan, tyrosine, and phenylalanine. Fluorescence of HSA is due mainly to tryptophan alone, because phenylalanine has a very low fluorescence quantum yield and the fluorescence of tyrosine is almost totally quenched if it is ionized or near an amino group, a carboxyl group, or a tryptophan residue.[22] Thus, intrinsic fluorescence of HSA is due mainly to the sole tryptophan residue (Trp-214) in the hydrophobic cavity of subdomain IIA (Sudlow I). Accordingly, if the probes bind in Sudlow site I, this may enhance fluorescence quenching of HSA. No fluorescence-quenching mechanism is expected to operate if the probes bind in the hydrophobic cavity of subdomain IIIA (Sudlow II) due to the probes' far location from Trp-214.

Figure 3 shows the overlap between the absorption spectra of 2Py, 3Py, and 4Py with the fluorescence spectrum of HSA. In the case of 2Py and 3Py, the overlaps are quite large. This is expected to enhance resonance energy transfer. Because of

(12) Abou-Zied, O. K.; Al-Shihi, O. I. K. *Proc. SPIE—Int. Soc. Opt. Eng.* **2008**, *6867*, 68670K–68670K12.
(13) Katritzky, A. R. *Physical Methods in Heterocyclic Chemistry*; Academic Press: New York, 1974.
(14) Albert, A.; Phillips, J. N. *J. Chem. Soc.* **1956**, *1*, 294–1304.
(15) Cox, R. H.; Bothner-By, A. A.; Aksel, A. *J. Phys. Chem.* **1969**, *73*, 2465–2468.
(16) Weisstuch, A.; Neidig, P.; Testa, A. C. *J. Lumin.* **1975**, *10*, 137–144.
(17) Metzler, D.; Snell, E. *J. Am. Chem. Soc.* **1955**, *77*, 2431–2437.
(18) Beak, P.; Convington, J. B. *J. Am. Chem. Soc.* **1978**, *100*, 3961–3963.
(19) Suradi, S.; El Saiad, N.; Pilcher, G.; Skinner, H. A. *J. Chem. Theromodyn.* **1982**, *14*, 45–50.
(20) Chevrier, M.; Guillerez, J.; Dubois, J. E. *J. Chem. Soc., Perkin Trans. 2* **1983**, 979–982.
(21) Putnam, F. W., Ed. *The Plasma Proteins*, 2nd ed.; Academic Press: New York, 1975; Vol. I, pp 133−181.
(22) Sułkowska, A. *J. Mol. Struct.* **2002**, *614*, 227–232.

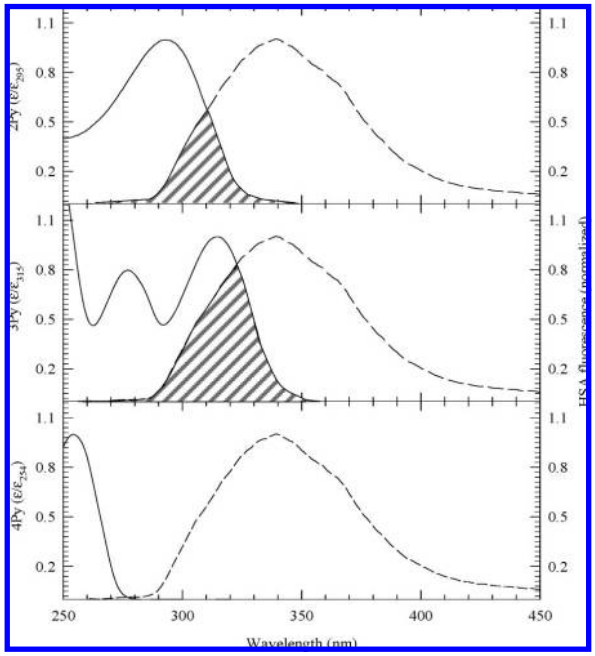

Figure 3. Overlap of the fluorescence spectrum of HSA (dashed line) with the absorption spectra (solid lines) of 2Py (first panel, $\varepsilon_{295} = 6965\ M^{-1}\ cm^{-1}$), 3Py (second panel, $\varepsilon_{315} = 3257\ M^{-1}\ cm^{-1}$), and 4Py (third panel, $\varepsilon_{254} = 13\,530\ M^{-1}\ cm^{-1}$). All solutions were prepared in a pH 7.2 sodium phosphate buffer. Concentrations of HSA and pyridones were 0.1 mM. $\lambda_{ex} = 280$ nm.

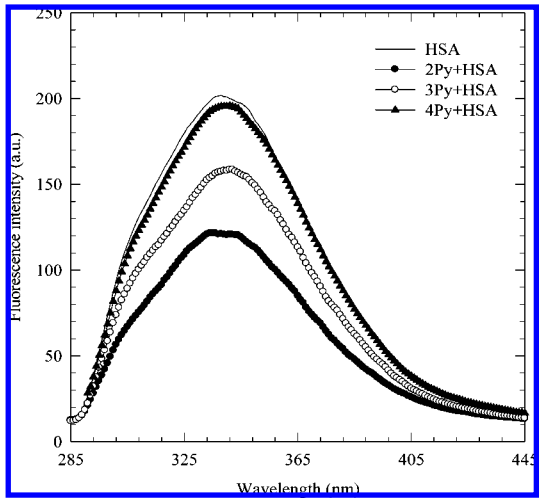

Figure 4. Quenching effect of 2Py, 3Py, and 4Py on the fluorescence spectrum of HSA. Concentrations of HSA and pyridones were 0.1 mM. $\lambda_{ex} = 280$ nm.

poor spectral overlap, no direct energy transfer was observed between HSA and 4Py at the concentrations of 4Py used in the present study. The molar extinction coefficient of 2Py in a buffer containing HSA was estimated at the maximum of the absorption peak to be $\varepsilon_{295} = 6965\ M^{-1}\ cm^{-1}$. For 3Py, the maximum absorption at 315 nm in buffer containing HSA was estimated to be $\varepsilon_{315} = 3257\ M^{-1}\ cm^{-1}$. The ε values indicate that 2Py may show more fluorescence-quenching effect than 3Py. This indeed was the observation as shown in Figure 4. In this figure, fluorescence of HSA was measured after excitation at 280 nm which represents the maximum absorption of the protein. Fluorescence of HSA was quenched more in the presence of 2Py than in the presence of 3Py. The measured fluorescence spectrum of HSA in the presence of 4Py shows almost no quenching, which is a result of the poor spectral overlap as mentioned above.

In order to confirm the steady-state observation, we measured the lifetime of HSA in the absence and presence of the probes. The Trp-214 residue in HSA is the main source of the fluorescence decay. Previous investigations have found that the lifetime of Trp-214 in normal HSA is heterogeneous. In most cases this heterogeneity was analyzed in terms of discrete exponential decays. Previously reported lifetimes of native HSA show two main components with a long decay in the range of 5.5−8.0 ns and a short component of 1.0−3.5 ns.[23–32] Our results for the decay of HSA are summarized in Table 1, and the transients are shown in the Supporting Information. The best fits for HSA were obtained using a biexponential function. The two time constants of HSA alone are 6.72 and 1.91 ns. Our results agree well with the above-mentioned values. We should point out that the contribution from the short component is small (<10%). In this regard, fitting the fluorescence decay to a monoexponential function yields reasonable fits, but the biexponential function better represents the overall decay as judged by the χ^2 values (Table 1). In the presence of 2Py, the two lifetimes of HSA were 6.31 and 0.98 ns, and in the presence of 3Py, the HSA lifetimes were 6.41 and 1.25 ns. Shorter lifetimes in the presence of 2Py are a manifestation of a stronger quenching mechanism than that in the presence of 3Py. In the presence of 4Py, the lifetimes of HSA were almost not affected (6.70 and 1.86 ns). The lifetime data show the same trend as observed in the fluorescence intensity change.

Quenching of the HSA fluorescence by 2Py or 3Py indicates that the probe molecules bind in Sudlow site I in subdomain IIA (see Figure 1). The distance between the donor (HSA) and acceptor (probe) can be calculated according to Förster's theory for resonance energy transfer (FRET).[33] The efficiency of energy transfer, E, is related to the distance (r_{AD}) between the donor (HSA) and acceptor (2Py or 3Py) by

$$E = \frac{R_0^6}{R_0^6 + r_{DA}^6} = 1 - \left(\frac{F}{F_0}\right) \quad (1)$$

where R_0 is the Förster distance (critical distance) when the efficiency of energy transfer is 50%. F and F_0 are the fluorescence intensities of HSA in the presence and absence of the quencher, respectively. The value of R_0 can be calculated from

$$R_0 = 0.211(\kappa^2 n^{-4} \varphi_D J)^{1/6} \quad (2)$$

where κ^2 is the spatial orientation factor between the emission dipole of the donor and the absorption dipole of the acceptor, n is the refractive index of the medium, ϕ_D is the fluorescence

(23) Helms, M. K.; Petersen, C. E.; Bhagavan, N. V.; Jameson, D. M. *FEBS Lett.* **1997**, *408*, 67–70.
(24) Davis, D. M.; McLoskey, D.; Brich, D. J. S.; Gellert, P. R.; Kit-tlety, R. S.; Swart, R. M. *Biophys. Chem.* **1996**, *60*, 63–77.
(25) Lakowicz, J. R.; Gryczynski, I. *Biophys. Chem.* **1992**, *45*, 1–6.
(26) Marzola, P.; Gratton, E. *J. Phys. Chem.* **1991**, *95*, 9488–9495.
(27) Vos, K.; van Hoek, A.; Visser, A. J. W. G. *Eur. J. Biochem.* **1987**, *165*, 55–63.
(28) Kasai, S.; Horie, T.; Mizuma, T.; Awazu, S. *J. Pharm. Sci.* **1987**, *76*, 387–392.
(29) Beechem, J. M.; Brand, L. *Annu. Rev. Biochem.* **1985**, *54*, 43–71.
(30) Hazan, G.; Haas, E.; Steinberg, I. Z. *Biochim. Biophys. Acta* **1976**, *434*, 144–153.
(31) Wahl, P.; Auchet, J. C. *Biochim. Biophys. Acta* **1971**, *285*, 99–117.
(32) De Lauder, W. B.; Wahl, P. *Biochem. Biophys. Res. Commun.* **1970**, *42*, 398–404.
(33) Förster, T., Sinanoglu, O., Eds. *Modern Quantum Chemistry*; Academic Press: New York, 1996; Vol. 3.

Table 1. Summary of Fluorescence Lifetime Measurements[a]

	double-exponential				single-exponential	
	τ_1 (ns)	τ_2 (ns)	$\langle\tau\rangle$ (ns)[b]	χ^2	τ (ns)	χ^2
HSA	6.72 ± 0.07 (0.93)	1.91 ± 0.26 (0.07)	6.38	0.95	6.41 ± 0.03	1.31
HSA + 2Py	6.31 ± 0.13 (0.95)	0.98 ± 0.20 (0.05)	6.04	0.87	6.05 ± 0.01	1.20
HSA + 3Py	6.41 ± 0.12 (0.95)	1.25 ± 0.18 (0.05)	6.15	0.96	6.20 ± 0.03	2.10
HSA + 4Py	6.70 ± 0.10 (0.92)	1.86 ± 0.20 (0.08)	6.31	0.99	6.40 ± 0.02	1.84
HSA + GdnHCl	3.47 ± 0.07 (0.88)	1.03 ± 0.10 (0.12)	3.30	0.91		
HSA + GdnHCl + 2Py	3.42 ± 0.05 (0.87)	0.76 ± 0.10 (0.13)	3.07	1.24		
HSA + GdnHCl + 3Py	3.46 ± 0.06 (0.90)	0.70 ± 0.10 (0.10)	3.18	1.12		
HSA + GdnHCl + 4Py	3.44 ± 0.01 (0.90)	1.01 ± 0.01 (0.10)	3.20	0.80		
L-tryptophan	3.86 ± 0.03 (0.90)[c]	0.55 ± 0.01 (0.10)[c]		1.05[c]	3.52 ± 0.02	1.10
L-tyrosine	3.16 ± 0.16 (0.79)	1.77 ± 0.31 (0.21)		0.84	2.78 ± 0.01	1.13

[a] Concentrations of HSA, pyridones, L-tryptophan, and L-tyrosine were 0.1 mM. The concentration of GdnHCl was 6.0 M. $\lambda_{ex} = 280$ nm. Emission was detected using Schott WG-305 and WG-320 filters. Relative contributions are listed in parentheses. [b] Average lifetime of τ_1 and τ_2. [c] Observed for $\lambda_{ex} = 295$ (using Schott WG-305 and WG-320 filters) and $\lambda_{ex} = 310$ nm (using Schott WG-320 filter).

quantum yield of the donor, and J is the overlap integral of the fluorescence emission spectrum of the donor and the absorption spectrum of the acceptor and is given by

$$J = \sum F(\lambda)\varepsilon(\lambda)\lambda^4 \frac{\Delta\lambda}{\sum F(\lambda)\Delta\lambda} \tag{3}$$

where $F(\lambda)$ is the fluorescence intensity of the donor at wavelength λ and $\varepsilon(\lambda)$ is the molar absorption coefficient of the acceptor at wavelength λ.

J can be evaluated by integrating the overlapped portion of the spectra in Figure 3. If both the donor and acceptor are tumbling rapidly and free to assume any orientation, then the dipole orientation factor, κ^2, equals 2/3.[34] In the present case, $n = 1.36$ and $\phi_D = 0.15$.[35] Using the aforementioned values, we calculated $R_0 = 1.75$ nm, $E = 0.315$, and $r_{AD} = 1.99$ nm for the HSA/2Py complex. The corresponding values for the HSA/3Py complex are $R_0 = 1.81$ nm, $E = 0.216$, and $r_{AD} = 2.24$ nm. The donor-to-acceptor distance in both complexes is less than 7 nm, indicating a static quenching interaction between the donor and acceptor according to Förster's nonradiative energy transfer theory.[33] When the calculated values for HSA/2Py are compared with those for HSA/3Py, the smaller E value and the larger r_{AD} value in the latter indicate lower energy transfer efficiency than in the former.

The operative quenching mechanism in the above complexes can be described by the Stern−Volmer quenching equation

$$\frac{F_0}{F} = 1 + k_q\tau_0[Q] = 1 + K_{SV}[Q] \tag{4}$$

where k_q is the quenching rate constant of the biomolecule, K_{SV} is the Stern−Volmer constant, τ_0 is the lifetime of the biomolecule (HSA) without the quencher, and [Q] is the quencher concentration. By varying the concentrations of 2Py and 3Py and keeping the HSA concentration fixed, k_q can be obtained from the slope of the regression curves of F_0/F versus [Q] as shown in Figure 5. For HSA/2Py, $k_q = 1.44 \times 10^{12}$ M^{-1} s^{-1}, and for HSA/3Py, $k_q = 3.45 \times 10^{11}$ M^{-1} s^{-1}. The calculated values of k_q are greater than the maximum dynamic collisional quenching constant of various kinds of quenchers with biopolymers.[36] The results confirm that a static quenching mechanism is operative in the present complexes. The larger value of k_q for the HSA/2Py complex compared to that for the HSA/3Py complex again indicates less quenching in the latter.

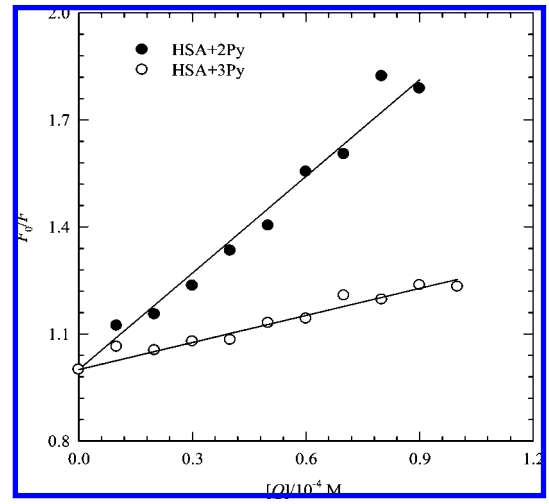

Figure 5. Stern−Volmer curves for quenching of HSA fluorescence by 2Py and 3Py.

For small molecules that bind independently to a set of equivalent sites in a macromolecule, the equilibrium between free and bound molecules is given by the equation[37]

$$\log\left[\frac{F_0 - F}{F}\right] = \log K + m \log[Q] \tag{5}$$

where K and m are the binding constant and the number of binding sites, respectively, and can be calculated by plotting $\log(F_0 - F/F)$ versus log[Q] as shown in Figure 6. The calculated values are $K = (3.4 \pm 0.4) \times 10^4$ M^{-1} and $m = 1.1$ for HSA/2Py and $K = (2.3 \pm 0.3) \times 10^4$ M^{-1} and $m = 1.1$ for HSA/3Py. The values of m indicate that in each case the probe is located in one binding site. The results, along with the quenching results, indicate that both probes, 2Py and 3Py, bind only in Sudlow site I in subdomain IIA and not in Sudlow site II (subdomain IIIA). Table 2 summarizes the calculated parameters.

Chemical Unfolding of HSA. A valuable feature of intrinsic protein fluorescence is the high sensitivity of tryptophan to its local environment. Changes in the emission spectra of tryptophan often occur in response to conformational transitions,

(34) Förster, T. *Discuss. Faraday Soc.* **1959**, *27*, 7–17.
(35) Cui, F. L.; Fan, J.; Ma, D.-L.; Liu, M.-C.; Chen, X.-G.; Hu, Z.-D. *Anal. Lett.* **2003**, *36*, 2151–2166.
(36) Ware, W. R. *J. Phys. Chem.* **1962**, *66*, 455–458.
(37) Connors, K. A. *Binding Constants. The Measurements of Molecular Complex Stability*; Wiley: New York, 1987.

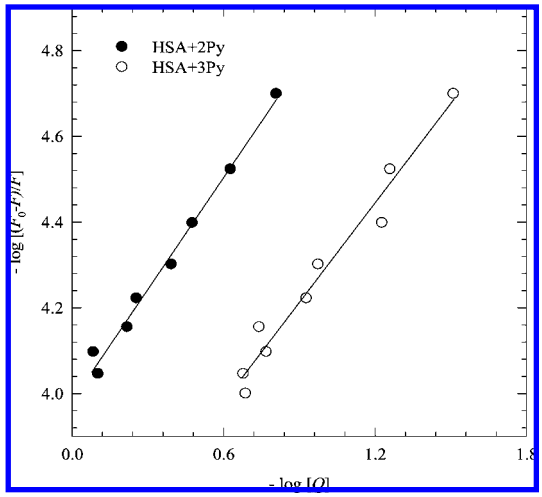

Figure 6. Plots of $-\log[(F_0 - F)]$ vs $-\log[Q]$ for HSA/2Py and HSA/3Py systems. The concentration of HSA was kept constant at 0.1 mM.

Table 2. Calculated Parameters for the HSA/2Py and HSA/3Py Complexes[a]

parameters	HSA/2Py	HSA/3Py
E	0.32	0.22
R_0 (nm)	1.75	1.81
r_{DA} (nm)	1.99	2.24
k_q (M^{-1} s^{-1})	1.44×10^{12}	3.45×10^{11}
K (M^{-1})	$(3.4 \pm 0.4) \times 10^4$	$(2.3 \pm 0.3) \times 10^4$
m	1.1	1.1

[a] Calculated using eqs 1–5. See text for details.

subunit association, substrate binding, or denaturation.[38] The latter can be induced chemically by using urea or GdnHCl. The chemical-induced denaturation changes in a protein molecule usually result in increased exposure of the protein chromophores (tryptophan, tyrosine, and phenylalanine residues) to water. This causes changes in their fluorescence. The most distinct changes occur in the case of tryptophan fluorescence in the form of a change in the fluorescence quantum yield and in a shift of the fluorescence spectrum toward longer wavelengths. In the case of tyrosine and phenylalanine fluorescence, protein denaturation results only in a change of the fluorescence quantum yield.[39]

The change in the HSA fluorescence was measured as a function of GdnHCl concentration after excitation at 280 nm. Figure 7 displays selected spectra. As the concentration of GdnHCl increases, the single peak starts to split into two peaks, a blue peak and a red peak. The change in fluorescence behavior is observable for GdnHCl concentration between 1.0 and 2.0 M, which indicates that the unfolding transition starts gradually and the maximum unfolding is reached for GdnHCl concentration of about 6.0 M. The results are in agreement with previous studies.[40–42]

The emission spectrum of native HSA shows a single peak with a maximum at 335 nm (Figure 7). The position of the peak indicates that the tryptophan residue is partially buried.[40] The

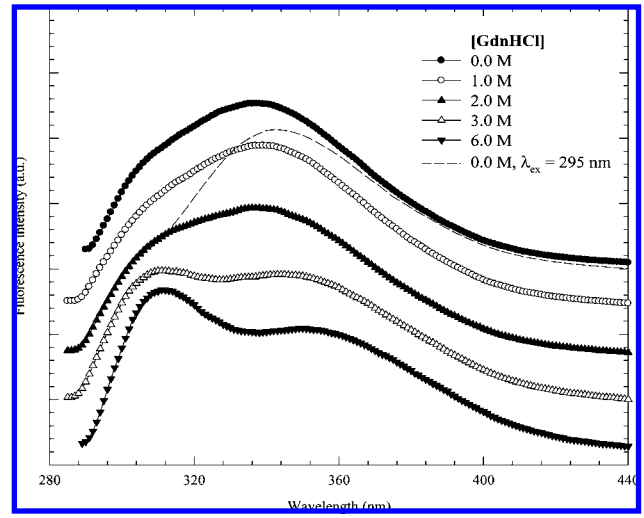

Figure 7. Fluorescence of HSA as a function of GdnHCl concentration. The concentration of HSA was 0.1 mM. $\lambda_{ex} = 280$ nm.

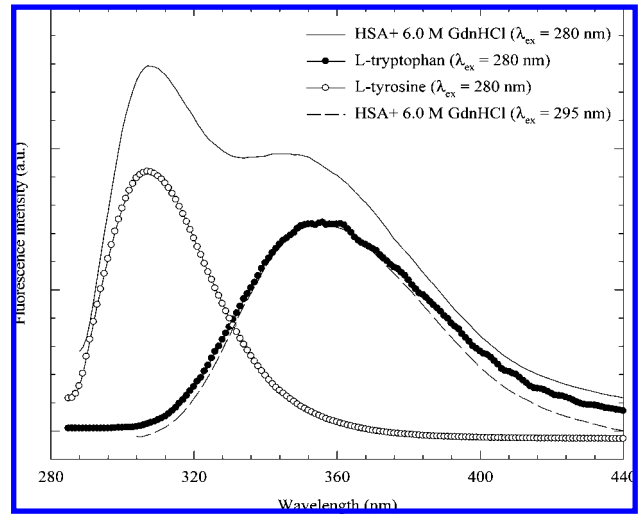

Figure 8. Fluorescence spectra of denatured HSA, L-tryptophan, and L-tyrosine. The concentration of HSA, L-tryptophan, and L-tyrosine was 0.1 mM in aqueous buffer. Excitation wavelength is indicated for each curve.

sensitivity of the fluorescence peak of tryptophan to environment polarity is a consequence of its large dipole moment in the excited state.[42] Tryptophans in fully or partially buried hydrophobic interiors or interfaces of proteins show blue-shifted emission anywhere from 309 nm in a fully buried environment to more typical 335 nm in a partially buried configuration. Trp-214 in HSA represents a typical case of a partially buried environment. In the presence of 6.0 M GdnHCl, two distinct peaks were observed at 308 and 355 nm (Figure 8). The peak at 355 nm is due to tryptophan emission in a polar environment which is confirmed by measuring the emission spectrum of L-tryptophan in buffer as shown in the figure. This result indicates that unfolding of HSA in the presence of 6.0 M GdnHCl is almost complete where the Trp-214 residue is fully exposed to the buffer.

On the other hand, HSA unfolding reduces quenching of tyrosine fluorescence.[43] In the native conformation, most of the tyrosine fluorescence is quenched as a consequence of the presence of nearby amino acids or the efficient energy transfer from the tyrosine fluorescence to Trp-214. Excitation of native

(38) Lakowicz, J. R. *Principles of Fluorescence Spectroscopy*; Springer: New York, 2006.
(39) Permyakov, E. A.; Burstein, E. A. *Biophys. Chem.* **1984**, *19*, 265–271.
(40) Santra, M. K.; Banerjee, A.; Rahaman, O.; Panda, D. *Int. J. Biol. Macromol.* **2005**, *37*, 200–204.
(41) Kamal, J. K. A.; Zhao, L.; Zewail, A. H. *Proc. Natl. Acad. Sci. U.S.A.* **2004**, *101*, 13411–13416.
(42) Kamal, J. K. A.; Behere, D. V. *Biochem.* **2002**, *41*, 9034–9042.

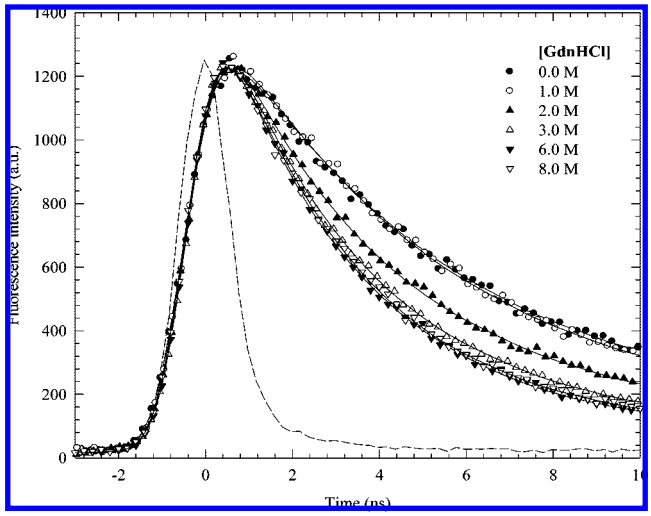

Figure 9. Fluorescence decay of HSA in aqueous buffer during the unfolding process as a function of GdnHCl concentration. $\lambda_{ex} = 280$ nm. Instrument response function (IRF) is shown by a dashed line. Solid lines represent the best fits to a biexponential function.

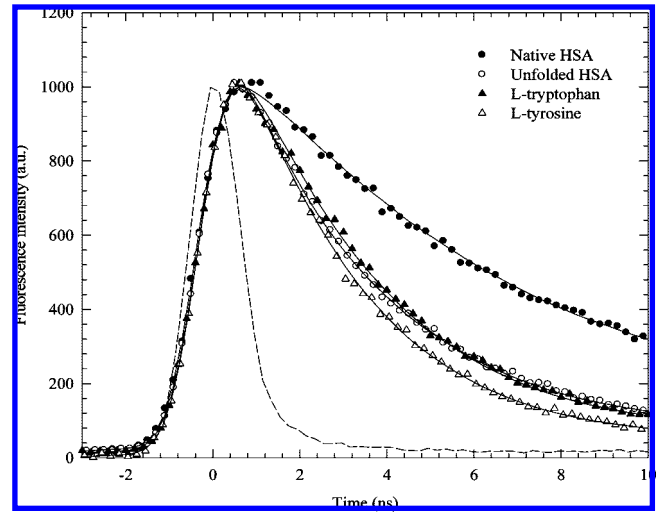

Figure 10. Fluorescence decay of native HSA, unfolded HSA, L-tryptophan, and L-tyrosine in aqueous buffer. $\lambda_{ex} = 280$ nm. IRF is shown by a dashed line. Solid lines represent the best fits to a biexponential function.

HSA at 280 nm results in a single fluorescence peak with a slight shoulder at 308 nm (Figure 7). Upon increasing the concentration of GdnHCl, this shoulder grows in intensity. Excitation at 295 nm should result in tryptophan fluorescence only, since tyrosine does not absorb in this region.[43] As shown in Figure 7, excitation at 295 nm produces only the tryptophan peak with no shoulder. The peak at 308 nm is then due to tyrosine fluorescence.

We confirmed the tyrosine assignment by measuring the fluorescence spectrum of L-tyrosine in buffer. The peak of L-tyrosine lies in the same spectral position of the blue peak (308 nm) as shown in Figure 8. We also measured the fluorescence of denatured HSA after excitation at 295 nm and observed only one fluorescence peak due to tryptophan (Figure 8). The enhancement of the tyrosine fluorescence in denatured HSA indicates that the local environment around one or more of the tyrosine residues has changed so that tyrosine fluorescence is possible. One possibility for this fluorescence can be the cessation of energy transfer from excited tyrosine to tryptophan with unfolding, when the distance between the tryptophan and the tyrosine residues increases. The spectra in Figure 7 show that changes in the fluorescence behavior can be used to follow protein unfolding.

The lifetime of HSA was measured as a function of GdnHCl concentration. Selected transients are shown in Figure 9. All transients were best fitted to a biexponential function. It is clear that fluorescence decay is faster as the GdnHCl concentration increases. The effect of denaturation on the slow decay component shows a lifetime reduction from 6.72 ns in native HSA to 3.47 ns in a complete unfolded HSA. The fast component changed from 1.9 to 1.03 ns, and its contribution was slightly increased. The results are included in Table 1. The change in the decay curves further confirms the steady-state results in which denaturation of HSA starts at GdnHCl concentration in the range of 1.0−2.0 M and is complete at [GdnHCl] ≥ 6.0 M.

In order to understand the effect of denaturation on the lifetimes of HSA, we must first discuss the origin of the two lifetime components. Since fluorescence in denatured HSA involves contribution from both tryptophan and tyrosine (Figure 8), we measured the fluorescence decay curves of L-tryptophan and L-tyrosine in buffer. The decays are shown in Figure 10, and the results are included in Table 1. Most of the reported data for tryptophan decay in water are in favor of two lifetimes of 3.1 and 0.5 ns, with difficulty in resolving the fast component.[38,44] The presence of rotamers was proposed to explain the two lifetime components. For tyrosine, the intensity decay in water is usually a single exponential, but different results were obtained at different observation wavelengths.[38,45] The dominant emission centered near 308 nm is responsible for a 3.40 ns component. A short lifetime component of 0.98 ns was assigned to tyrosinate which forms during the excited-state lifetime, centered near 360 nm.

We observed one lifetime of 3.52 ns for L-tryptophan after excitation at 280 nm. Two components (3.86 and 0.55 ns) were only observed after excitation at longer wavelengths (295 and 310 nm). For L-tyrosine, the best fit yields two lifetimes of 3.16 and 1.77 ns after excitation at 280 nm.

The measured lifetimes of tryptophan and tyrosine in buffer are similar. This makes it very difficult to resolve the contributions from each one in unfolded HSA, especially when other factors affect their decay components inside HSA such as dynamic processes occurring during the excited-state lifetime. These dynamic processes can include nearby motion of quenchers, spectral relaxation, and/or resonance energy transfer.[46,47] The two decay components for unfolded HSA are very close to those measured for tryptophan and tyrosine in buffer (Table 1 and Figure 10). For excitation at 280 nm, it was not possible experimentally to separate the tyrosine fluorescence contribution from that of tryptophan due to the overlap of the two fluorescence bands. In order to avoid contribution from tyrosine to the total fluorescence decay of unfolded HSA, we measured the decay curves after excitation at 295 and 310 nm where

(43) Gorinstein, S.; Goshev, I.; Moncheva, S.; Zemser, M.; Weisz, M.; Caspi, A.; Libman, I.; Tzvi Lerner, H.; Trakhtenberg, S.; Martin-Belloso, O. J. *Protein Chem.* **2000**, *19*, 637–642.
(44) Beechem, J. M.; Brand, L. *Annu. Rev. Biochem.* **1985**, *54*, 43–71.
(45) Guzow, K.; Ganzynkowicz, R.; Rzeska, A.; Mrozek, J.; Szabelski, M.; Karolczak, J.; Liwo, A.; Wiczk, W. *J. Phys. Chem. B* **2004**, *108*, 3879–3889.
(46) Tanaka, F.; Mataga, N. *Biophys. J.* **1987**, *51*, 487–495.
(47) Alcala, J. R. *J. Chem. Phys.* **1994**, *101*, 4578–4584.

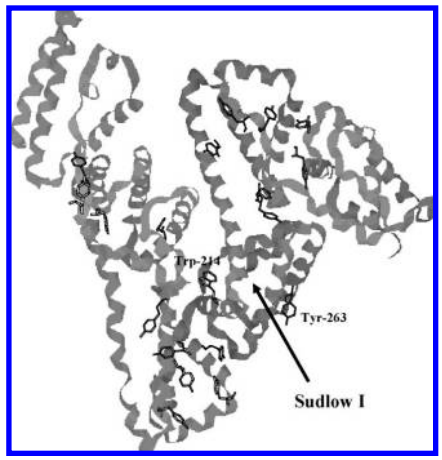

Figure 11. Crystal structure of HSA with the locations of the 18 Tyr residues. The locations of Trp-214 and Tyr-263 residues in the Sudlow I binding site are marked. The structure was obtained from the Protein Data Bank (ID code 1ha2).

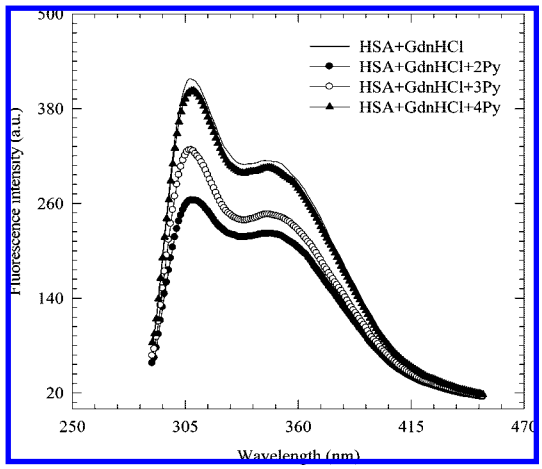

Figure 12. Quenching effect of 2Py, 3Py, and 4Py on the fluorescence spectrum of unfolded HSA. Concentrations of HSA and pyridones were 0.1 mM in phosphate buffer. GdnHCl concentration was 6.0 M. $\lambda_{ex} = 280$ nm.

absorption is only due to tryptophan. We observed no change in the decay behavior when compared to those measured after excitation at 280 nm. This observation indicates that the measured lifetimes in native and denatured HSA are typical of tryptophan relaxation. Comparison of the measured lifetimes in the unfolded state of HSA with those of tryptophan in buffer indicates that complete unfolding of subdomain IIA exposes the Trp-214 residue to solvent as observed in the steady-state fluorescence measurements (Figure 8).

From the X-ray structure of HSA shown in Figure 1, we identified the number and location of tyrosine residues in native HSA. Figure 11 displays the results. There are 18 Tyr residues in HSA. Their locations are distributed in HSA as indicated in the figure. Even after denaturation, fluorescence from many of the tyrosine residues may still suffer from complete quenching if the nearby amino acids act as energy acceptors.

We investigated the above point by using the three pyridones as probes in denatured HSA. The addition of the three probes to denatured HSA results in a decrease in the fluorescence intensity of both tryptophan and tyrosine as shown in Figure 12. As in the case of native HSA, 4Py shows very little quenching because its absorption spectrum does not overlap with

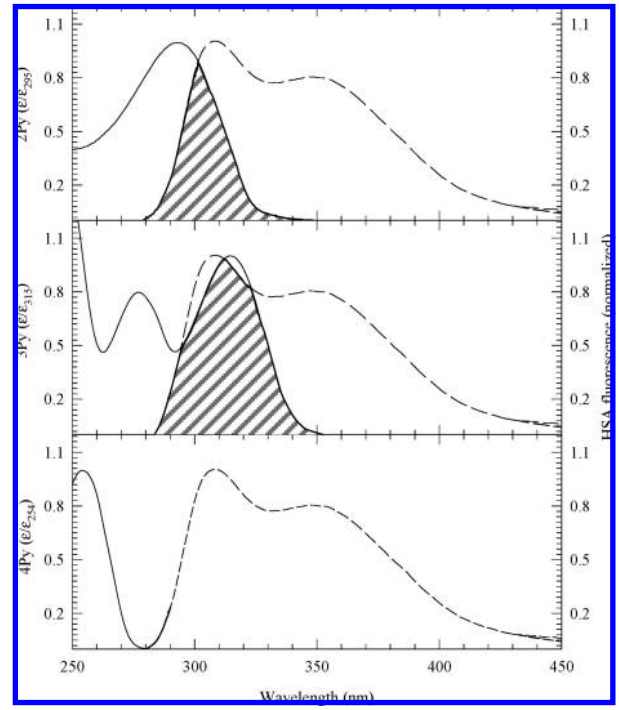

Figure 13. Overlap of the fluorescence spectrum (dashed line) of unfolded HSA ($\lambda_{ex} = 280$ nm) with the absorption spectra (solid lines) of 2Py (first panel, $\varepsilon_{295} = 6965\ M^{-1}\ cm^{-1}$), 3Py (second panel, $\varepsilon_{315} = 3257\ M^{-1}\ cm^{-1}$), and of 4Py (third panel, $\varepsilon_{254} = 13\,530\ M^{-1}\ cm^{-1}$). All solutions were prepared in phosphate buffer. Concentrations of HSA and pyridones were 0.1 mM. GdnHCl concentration was 6.0 M.

the emission spectrum of denatured HSA (Figure 13). On the other hand, the overlaps between the absorption spectra of 2Py and 3Py with the fluorescence spectrum of denatured HSA are quite large as shown in Figure 13.

The results indicate that, after denaturation, Trp-214 is still close to the probes so that its fluorescence is quenched to some extent. Although no crystal structures of HSA in such denatured or unfolded states are available, the quenching results may point to the fact that the location of Trp-214 in subdomain IIA did not change much compared to its location in native HSA and that denaturation only exposes Trp-214 to the solvent. For the case of tyrosine, quenching of its fluorescence in the presence of 2Py and 3Py indicates that most likely fluorescence in this case is due mainly to one nearby Tyr in subdomain IIA. By considering the locations of the tyrosine residues shown in Figure 11, the closest tyrosine to Sudlow site I is the Tyr-263 residue. The location of this residue is in subdomain IIA, close to the binding site and not completely buried inside the protein. Tyr-263 may be one of the residues responsible for the shoulder at 308 nm in the fluorescence spectrum of native HSA (Figure 7). Upon denaturation, Tyr-263 will most likely be exposed to solvent and farther from Trp-214. Such conditions explain the observed enhancement in tyrosine fluorescence.

Lifetime measurements of denatured HSA in the presence of the probes are included in Table 1. Although the decrease in lifetimes is within the measured uncertainty, the trend is similar to that observed in the steady-state fluorescence.

Dilution Refolding of HSA. Refolding of HSA after denaturation by GdnHCl was performed by dilution with buffer. The completely unfolded HSA (100 μM) at 6.0 M GdnHCl was diluted to a final concentration of 2 μM, where the GdnHCl concentration was 0.1 M. Fluorescence of HSA was monitored

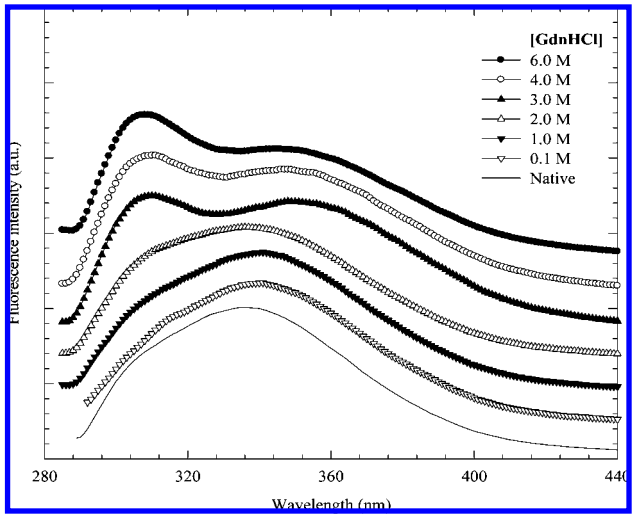

Figure 14. Fluorescence of HSA in aqueous buffer during the refolding process as a function of GdnHCl concentration after dilution. $\lambda_{ex} = 280$ nm.

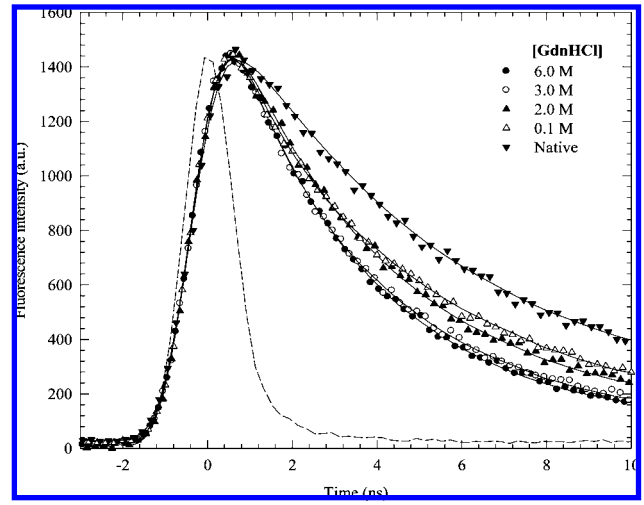

Figure 15. Fluorescence decay of HSA in aqueous buffer during the refolding process as a function of GdnHCl concentration after dilution. $\lambda_{ex} = 280$ nm. IRF is shown by a dashed line. Solid lines represent the best fits to a biexponential function.

during the process of dilution. During the course of refolding, we compared the steady-state fluorescence of HSA after each dilution step with that of native HSA. Selected spectra are shown in Figure 14.

As the concentration of GdnHCl decreases by dilution, the two fluorescence peaks due to tyrosine and tryptophan start to merge and form a single peak. This result indicates that refolding brings the protein close to its native state. If the refolding process is completely reversible, the fluorescence peak at 0.1 M GdnHCl should match that of the native HSA. As shown in Figure 14, the shape of the peak at such concentration of GdnHCl shows the characteristics of a folded HSA, but a small red-shift of the Trp-214 fluorescence from that in the native HSA is clearly observed (~5 nm). This observation indicates that the Trp-214 residue in the refolded HSA is partially exposed to a polar environment.

The steady-state results were confirmed by measuring the lifetimes of HSA during the process of refolding. Selected transients are shown in Figure 15. The decay curves were best fitted to a biexponential function for each step of dilution. As refolding progresses by dilution, the two lifetimes of HSA show values which move toward the values of the native state of HSA. However, extreme dilution of denatured HSA ([HSA] = 2 μM and [GdnHCl] = 0.1 M) produces a decay curve with two lifetimes of 5.77 ± 0.11 and 1.09 ± 0.07 ns. These values indicate that refolding is not complete (compared to 6.72 ± 0.07 and 1.91 ± 0.26 ns for native HSA).

The above results reflect the refolding of domain IIA which contains both Tyr-263 and Trp-214. Refolding of HSA domains was found to follow a stepwise fashion where refolding of domain II occurred slower than refolding of domains I and III.[40] Mitra et al.[48] reported a thermal unfolding/cooling refolding experiment of HSA. The authors report that after unfolding at 70 °C, domain IIA is exposed to an aqueous environment, resulting in the swelling of the protein to a higher hydrodynamic diameter so that water will still exist in the domain after refolding. Hydration of the amino acids in domain IIA after unfolding may overcome the hydrophobic force so that recovery of the native orientation of the amino acids will not be achieved by refolding. This case of irreversible refolding becomes partial when cooling refolding was performed after HSA was induced to unfold thermally up to 55 °C. The authors report a complete reversible refolding when heating was up to 50 °C. Our results support the concept of a partial refolding mechanism which hinders a full recovery from the denatured state.

Finally, the above stepwise unfolding and refolding experiments were performed in the presence of 2Py and 3Py, and no additional changes were observed rather than a decrease in the fluorescence intensity due to quenching (results are shown in the Supporting Information). This indicates that the small probes maintain their binding to HSA during the processes of unfolding and refolding with no noticeable effects on the protein structure.

Conclusions

The mechanism of binding of 2Py, 3Py, and 4Py to HSA was investigated using steady-state and lifetime fluorescence measurements. Quenching of HSA fluorescence was found to be a function of the amount of spectral overlap between the donor's fluorescence and acceptor's absorption where only 2Py and 3Py cause a reduction in the fluorescence intensity and lifetime of HSA. This observation indicates that subdomain IIA binding site (Sudlow site I) is the host of the probes and the reduction in fluorescence of HSA is due to energy transfer from the Trp-214 residue to the probe in each case. The distance between Trp-214 and each of the probes was calculated using Förster theory for energy transfer to be 1.99 nm for HSA/2Py and 2.44 nm for HSA/3Py. The shorter distance in the former complex indicates more efficient energy transfer than in the latter. This was confirmed by estimating the quenching rate constant and binding constant in each complex. The results indicate a static quenching mechanism operating in the two complexes. The number of binding sites of both complexes was also estimated to be one which indicates that both probes bind only in Sudlow site I.

Chemical unfolding of HSA was studied at different concentrations of GdnHCl. Unfolding started at [GdnHCl] > 1.0 M, whereas a complete unfolding was achieved at [GdnHCl] ≥ 6.0 M. Upon unfolding, two fluorescence peaks were observed. One peak was assigned to the Trp-214 residue in a

(48) Mitra, R. K.; Sinha, S. S.; Pal, S. K. *Langmuir* **2007**, *23*, 10224–10229.

polar environment, and the other peak was assigned to tyrosine fluorescence. Fluorescence quenching of the two peaks after probe binding indicates that one of the tyrosine residues responsible for fluorescence is Tyr-263 which is located in subdomain IIA close to the binding site. The measured lifetimes of denatured HSA are typical of tryptophan in a polar environment. Dilution of denatured HSA results in a partial refolding of subdomain IIA which is attributed to a degree of swelling of the binding site caused by water. This swelling hinders a complete refolding from the denatured state.

Acknowledgment. This work was supported by the Sultan Qaboos University (Grant No. IG/SCI/CHEM/05/03).

Supporting Information Available: Fluorescence decay transients of HSA with and without the probes, fluorescence spectra of HSA with and without the probes during the processes of unfolding and refolding. This material is available free of charge via the Internet at http://pubs.acs.org.

JA8031289